Physiologia Plantarum 128: 237–250. 2006

Using quantitative proteomics of *Arabidopsis* roots and leaves to predict metabolic activity

Brian P. Mooney[a,b], Jan A. Miernyk[a,c], C. Michael Greenlief[b,d] and Jay J. Thelen[a,*]

[a]Department of Biochemistry, University of Missouri, Columbia, 109 Life Science Center, Columbia, MO 65211, USA
[b]Charles W. Gehrke Proteomics Center, 109 Life Sciences Center, 1201 E. Rollins St., Columbia, MO 65211, USA
[c]USDA, Agricultural Research Service, Plant Genetics Research Unit, Columbia, MO 65211, USA
[d]Department of Chemistry, 125 Chemistry Building, 601 S. College Ave, Columbia, MO 65211, USA

Correspondence
*Corresponding author,
e-mail: thelenj@missouri.edu

Received 14 March 2006; revised 31 March 2006

doi: 10.1111/j.1399-3054.2006.00746.x

Proteins isolated from developing roots and leaves of *Arabidopsis thaliana* were separated by high-resolution two-dimensional (2-D) electrophoresis. The resulting 2-D proteome maps are markedly different. Quantitative analysis of root and leaf protein spot pairs revealed that in most instances there was at least a 1.5-fold differential. Peptide mass fingerprint analysis of the 288 most abundant 2-D spots from each organ allowed 156 and 126 protein assignments for roots and leaves, respectively, 54 of which were common. Metabolism-related proteins accounted for 20% of assignments in samples from both organs, whereas energy-related proteins comprised 25 and 18% of leaf and root samples, respectively. Proteins involved in disease resistance and defense encompass 13% of root proteins, but only 7% of leaf proteins. Comparison of protein abundance with transcript abundance, using previously reported microarray data, yielded a correlation coefficient of approximately 0.6, suggesting that it is inappropriate to make protein level or metabolic conclusions based solely upon data from transcript profiling. A comparative model of root and leaf metabolism was developed, based upon protein rather than transcript abundance. The model indicates elevated one-carbon and tricarboxylic acid metabolism in roots relative to leaves.

Introduction

Plants perform a myriad of functions essential for growth and development, most within specialized organs. For example, leaves are responsible for light harvesting and carbon fixation, whereas roots absorb water and nutrients from the soil (Kochian 2000, Malkin and Niyogi 2000). Roots are composed of rapidly dividing tissues that are non-photosynthetic, and therefore require sucrose from the source leaves. The fundamental differences between

Abbreviations – 2-D, two-dimensional; CBB, Coomassie brilliant blue; cDNA, complementary DNA; CHAPS, 3-[(3-cholamidopropyl) dimethylammonio]-1-propanesulfonate; DIGE, difference gel electrophoresis; DTT, dithiothreitol; IEF, isoelectric focusing; IPG, immobilized pH gradient; MALDI-TOF, matrix-assisted laser desorption ionization time-of-flight; MOWSE, Molecular Weight Search; MS, mass spectrometry; PMF, peptide mass fingerprint; RuBisCO, ribulose-1,5-bisphosphate carboxylase oxygenase; SDS-PAGE, sodium dodecyl sulfate–polyacrylamide gel electrophoresis; Vh, volt hours.

This investigation was supported by United States Department of Agriculture – National Research Initiative grant 2003-00659 (J.J.T.) and National Science Foundation Young Investigator Award DBI-0332418 (J.J.T.). Any opinions, findings and conclusions expressed in this manuscript are those of the author(s) and do not necessarily reflect the views of the National Science Foundation or US Department of Agriculture.

roots and leaves necessitate a high level of developmental, structural and metabolic divergence that has frequently been observed (Byrne 2005, Ueda et al. 2005) but infrequently analyzed or compared in a systematic manner, particularly at the protein level.

Anonymous profiling of protein expression has entered a new era embodied by recent improvements in protein separation and mass spectral instrumentation. Current high-resolution two-dimensional (2-D) electrophoresis, using immobilized pH gradient (IPG) strips, allows greater control over reproducibility and protein sample loading (Görg et al. 2004). The latter is particularly important because the vast dynamic range of protein expression is commonly an obstacle to in-depth proteome investigations of both plants and animals. The preponderance of low turnover or sequestered proteins hinders profiling of low-abundance polypeptides, particularly when using earlier generation, low-resolution capillary isoelectric focusing (IEF) methods (Görg et al. 2004, Hajduch et al. 2005). Current high-resolution 2-D electrophoresis is frequently coupled with peptide mass fingerprint (PMF) identification (Pappin et al. 1993), through matrix-assisted laser desorption ionization time-of-flight (MALDI-TOF) mass spectrometry (MS). The low polypeptide complexity of 2-D gel spots simplifies the challenge of protein assignment from MS spectra. Although greatly facilitated by complete and accurate gene or complementary DNA (cDNA) sequence data, PMF identification has nevertheless been validated for a number of plants, which do not yet have completely sequenced genomes including *Medicago truncatula* (Watson et al. 2003), *Zea mays* (Porubleva et al. 2001) and *Glycine max* (Hajduch et al. 2005, Mooney et al. 2004).

In recent years, *Arabidopsis thaliana* has become the reference plant used to address complex biological questions. Small stature, rapid growth cycle and ease of transformation are characteristics that have made *A. thaliana* the organism of choice for many plant biologists (Somerville and Koornneef 2002). As the only dicot plant with a fully sequenced genome, it is also a reference for proteome investigations (Agrawal et al. 2004). The low redundancy of the *A. thaliana* genome (*Arabidopsis* Genome Initiative 2000) is also advantageous for in-depth proteome investigations. Previous proteomic investigations of roots and leaves from *M. truncatula* (Watson et al. 2003) and rice (Komatsu and Tanaka 2004), and leaves from maize (Porubleva et al. 2001) and *A. thaliana* (Giavalisco et al. 2005), have provided the identification of approximately 100 of the most abundant proteins. Identification of the predominant proteins expressed in roots of *A. thaliana* will help to extend our understanding of these prominent and functionally distinct organs. Furthermore, we propose using results from gel-based quantitative proteomic analyses as a basis for comparative metabolic modeling.

Materials and methods

Plant material

Seeds of *A. thaliana* L. var. Columbia were sown in moistened Pro-mix soil and grown at 20°C with a 16-h light cycle under low light condition (40–50 μmol photon m^{-2} s^{-1}). Whole root balls were harvested from soil-grown *A. thaliana* plants exactly 3 weeks after germination. Roots were carefully rinsed in water to remove soil prior to protein isolation. Primary leaves were harvested 4 h into a light cycle exactly 3 weeks after germination.

Protein isolation from plant organs

Proteins were isolated from organs using a procedure modified from Hurkman and Tanaka (1986). Plant organs (approximately 1 g) were pulverized to a fine powder in a mortar and pestle in the presence of liquid N_2. Powder was resuspended directly in the mortar with 15 ml of homogenization media [50% phenol, 0.45 *M* sucrose, 5 m*M* ethylenediaminetetraacetic acid, 0.2% (v/v) 2-mercaptoethanol, 50 m*M* Tris–HCl, pH 8.8] with continued grinding until the homogenate reached room temperature. Samples were transferred to phenol-resistant screw-cap tubes and incubated on a Nutator mixer for 30 min at 4°C, then centrifuged 5000 *g* for 15 min at 4°C in a swinging-bucket rotor. The upper, phenol-phase was removed and added to five volumes of ice-cold 0.1 *M* ammonium acetate in 100% methanol, then mixed before placing at −20°C for a minimum of 1 h. Precipitated proteins were collected by centrifugation (10 min at 5000 *g*) and supernatants decanted. Pellets were thoroughly washed twice with 20 ml of 0.1 *M* ammonium acetate in 100% methanol followed by two washes with ice-cold 80% acetone, and a final wash in ice-cold 70% ethanol. Washed pellets were either stored at −20°C or dissolved immediately for IEF.

Sample preparation for difference gel electrophoresis

Protein pellets were dissolved in difference gel electrophoresis (DIGE) sample buffer [30 m*M* Tris–HCl, pH 8.5, 7 *M* urea, 2 *M* thiourea, 4% 3-[(3-cholamidopropyl) dimethylammonio]-1-propanesulfonate (CHAPS)], by gentle vortexing for 1 h at room temperature. Insoluble material was sedimented at 14 000 *g* for 20 min. Supernatants were decanted and protein concentrations

determined by the dye-binding assay (BioRad, Hercules, CA). Each sample (50 μg protein) was then labeled with the charge-matched, N-hydroxysuccinimide (NHS)-activated cyanine dyes according to the manufacturer's instructions (GE Healthcare/Amersham Biosciences, Piscataway, NJ) with the following modifications. Each 50 μg protein sample was adjusted to 10 μl final volume by addition of sample buffer. One microliter (100 pmol) of the appropriate dye (Cy3 or Cy5) was then added to the protein sample, and labeling conducted on ice for 30 min. Labeling was terminated, and excess dye quenched by the addition of 10 m*M* L-lysine followed by incubation on ice for a further 10 min. Dithiothreitol (DTT) was added to a final concentration of 60 mM and samples were incubated on ice for an additional 10 min. The Cy3 and Cy5 samples were then combined and the volume was adjusted to 420 μl by the addition of IEF rehydration buffer [8 *M* urea, 2 *M* thiourea, 2% (w/v) CHAPS, 2% (w/v) Triton X-100, 50 m*M* DTT, 2 m*M* tributyl phosphine, 0.5% (v/v) carrier ampholytes]. The IPG strips, 24 cm, pH 4–7 (GE Healthcare/Amersham Biosciences, Piscataway, NJ) were passively rehydrated with the cyanine dye–labeled samples for 2 h. The IEF protocol, which included active strip rehydration for 12 h at 50 V, was conducted using the Protean IEF Cell from BioRad (Hercules, CA) with the following focusing protocol: 500 V for 500 volt hours (Vh), 1000 V for 1000 Vh and 8000 V for 90 000 Vh. The IPG strips were then processed for sodium dodecyl sulfate–polyacrylamide gel electrophoresis (SDS-PAGE).

Preparative IEF

Protein pellets were dissolved in 2 ml of IEF rehydration buffer by pipetting followed by vortex mixing (1 h at 10% maximum). Insoluble matter was removed by centrifugation for 20 min at 14 000 *g*, and supernatants were transferred to separate tubes. Protein concentrations were determined using 0.5–2 μl of sample to minimize interference from high concentrations of detergent and reductant. Protein quantitation was performed in triplicate, and compared with a standard curve prepared from chicken gamma-globulin. Exactly 1.0 mg of protein was added to separate tubes and volumes were brought up to 0.42 ml with IEF rehydration buffer. The IEF was conducted under the same conditions as those used for the cyanine dye–labeled samples.

SDS-PAGE for 2-D electrophoresis

Following IEF, the IPG strips were removed from the focusing tray and blotted on Kimwipes to remove mineral oil. The strips were then incubated in equilibration buffer [50 m*M* Tris–HCl, pH 6.8, 6 *M* urea, 30% (v/v) glycerol, 5% (w/v) SDS] plus 2% (w/v) DTT for 15 min with gentle agitation, followed by incubation in buffer supplemented with 2.5% (w/v) iodoacetamide for 15 min with gentle agitation. The IPG strips were then rinsed with SDS-PAGE running buffer and placed onto 11–17% linear gradient acrylamide gels. Strips were then overlaid with agarose solution [60 m*M* Tris–HCl, pH 6.8, 60 m*M* SDS, 0.5% (w/v) agarose, 0.01% (w/v) bromophenol blue]. Second dimension SDS-PAGE was conducted in a Dalt 6 electrophoresis unit (GE Healthcare/Amersham Biosciences) for 5 h at 100 W constant power (six gels). Following SDS-PAGE gels were washed three times for 15 min with deionized H_2O, then stained for 16 h with colloidal Coomassie brilliant blue (CBB) [20% (v/v) ethanol, 1.6% (v/v) phosphoric acid, 8% (w/v) ammonium sulfate, 0.08% (w/v) CBB G-250].

Image capture and analysis of 2-D gels of cyanine dye–labeled proteins

The 2-D gels of cyanine dye–labeled protein samples were removed from the glass plates and washed in water for 10 min immediately after electrophoresis. Washed gels were placed directly on the imaging plate of a dual photomultiplier tube laser-imaging instrument (FLA5000, Fuji Medical, Stamford, CT) to collect two channels of data (i.e. Cy3 and Cy5). Images of Cy3- and Cy5-labeled proteins were acquired in a single scan at 16-bit pixel depth and 50 μm resolution. Image analysis was performed using the Difference In-gel Analysis program of the DeCyder software suite (GE Healthcare/Amersham Bioscience). Spot detection, background subtraction, normalization and matching were each performed on raw TIFF images using default settings. Initial spot detection settings were for 1300 total spots, followed by an exclude filter for spots with slope >2 and area <150.

Image analysis, spot excision and tryptic digestion of proteins

Electronic images of CBB-stained, 2-D gels were analyzed using Phoretix 2D-Advanced software (Nonlinear Dynamics, Newcastle, UK). Spot detection, background subtraction and spot quantitation were performed on true 16-bit TIFF images acquired with a scanning densitometer. Background subtraction on detected spots was performed using the mode of non-spot function. Protein spots were excised and arrayed into 96-well MultiScreen model R5, 5 μ*M* hydrophilic polytetrafluoroethylene membrane glass-filled polypropylene plates (Millipore, Bedford, MA) using 1.4-mm diameter pins on the GelPix robotic spot excision station (Genetix Ltd., UK).

Gel plugs were destained in 200 μl of 50% (v/v) acetonitrile, 50 m*M* ammonium bicarbonate, and incubated at 25°C for 30 min. Destaining solution was evacuated from the bottom of the filter plates using a vacuum manifold designed for MultiScreen plates (Millipore, Bedford, MA). Destaining was repeated until the blue color was removed from the samples (typically twice). Gel plugs were dehydrated in 100% acetonitrile for 5 min at room temperature. Acetonitrile was evacuated from the plates using a vacuum manifold and the underside of plates was gently blotted onto filter paper to remove residual solvent. Sequencing grade trypsin (20 μg, Promega, Madison, WI) was thoroughly resuspended in 5 ml of 50 m*M* ammonium bicarbonate, and 50 μl was added to each well. Adhesive tape was placed over the wells, a 96-well V-bottom sample collection plate was placed underneath the MultiScreen plates (to collect any liquid) and the samples were incubated at 37°C for 16 h. Tryptic peptides were extracted from gel plugs with 50 μl of 60% (v/v) acetonitrile, 0.3% (v/v) trifluoroacetic acid, with gentle agitation in a microplate shaker (140 rpm) for 15 min and collected into a V-well collection plate using a vacuum evacuation manifold. Samples were concentrated to 5–15 μl by centrifugal vacuum evaporation.

Mass determination of tryptic peptides

Tryptic peptide samples (0.5 μl) were applied to a 96 × 2 Teflon MALDI plate using a Symbiot I liquid-handling station (Applied Biosystems, Foster City, CA). The samples were mixed on-target with an equal volume of the matrix solution, 10 mg ml^{-1} α-cyano-4-hydroxycinnamic acid (Sigma–Aldrich Fluka, St. Louis, MO) prepared in 60% (v/v) acetonitrile, 0.3% (v/v) trifluoroacetic acid. Analyses of trypsin-digested samples were carried out using a Voyager-DE PRO MALDI-TOF MS (Applied Biosystems, Foster City, CA), operated in the positive ion delayed extraction reflector mode for highest resolution and mass accuracy. Peptides were ionized/desorbed with a 337-nm laser and spectra were acquired at 20-kV accelerating potential with optimized parameters. The close external calibration method using a mixture of standard peptides (Applied Biosystems) provided mass accuracy of 25–50 ppm across the mass range of 700–4500 Da.

PMF database mining and validation of protein assignments

Peptide spectra were automatically processed for baseline correction, noise removal, peak deisotoping and threshold adjustment (2% base peak intensity) prior to submission to a local copy of version 3.2.1 of the MS Fit program of Protein Prospector (http://prospector.ucsf.edu) to search the NCBInr *A. thaliana* database. Search criteria required the match of at least four peptides with a mass error of less than 100 ppm, and one missed cleavage was allowed. Oxidation of Met, N-terminal acetylation, and pyro-Glu was set as variable modifications, whereas carbamidomethyl modification of Cys residues was set as a fixed modification. Tentative protein assignments required a minimum Molecular Weight Search (MOWSE) score of 130 and a minimum of 10% protein sequence coverage. Theoretical and experimental (from 2-D gel) protein masses were required to be within 25% variance. These thresholds are more stringent than both the manufacturer's recommendations and most published recommendations, and probably resulted in discarding many potentially valid protein assignments. Indeed, we were able to successfully identify protein standards with fewer than four peptides and MOWSE scores below 100 using the current workflow (data not shown).

Results

2-D gel analysis of roots and leaves reveals fundamental differences in protein expression

High-resolution 2-D electrophoresis of *A. thaliana* root and leaf samples revealed over 400 CBB-stained proteins in each gel in the pH range 4–7 (Fig. 1). Quantification of spot volumes indicated that the dynamic range of protein expression in leaves was at least 120-fold, as compared with roots where it was approximately 30-fold. The higher dynamic range in leaves is because of the preponderance of ribulose-1,5-bisphosphate carboxylase oxygenase (RuBisCO) large and small subunits, spots 14, 28, 31, 32, 34–40, and spots 127, 128, respectively. The 2-D gel maps from the two organs are markedly different, which confounded both manual and computer-assisted spot matching. To improve the accuracy of spot matching, DIGE was performed for sample multiplexing. Exactly 50 μg of protein from roots and leaves was labeled with Cy3 or Cy5 dyes, respectively, using primary amine reactive conjugation chemistry (Fig. 2A). After labeling, unreacted dye was quenched with lysine, the samples were pooled and then resolved by 2-D electrophoresis (Fig. 2A). Because the samples were pooled prior to gel electrophoresis, protein spot matching was simplified by eliminating gel-to-gel variation. In agreement with CBB-stained 2-D gels, the overall spot pattern indicates fundamental protein expression differences between roots and leaves, clearly visualized after false color assignment (Fig. 2B, upper panel). Analysis of root and

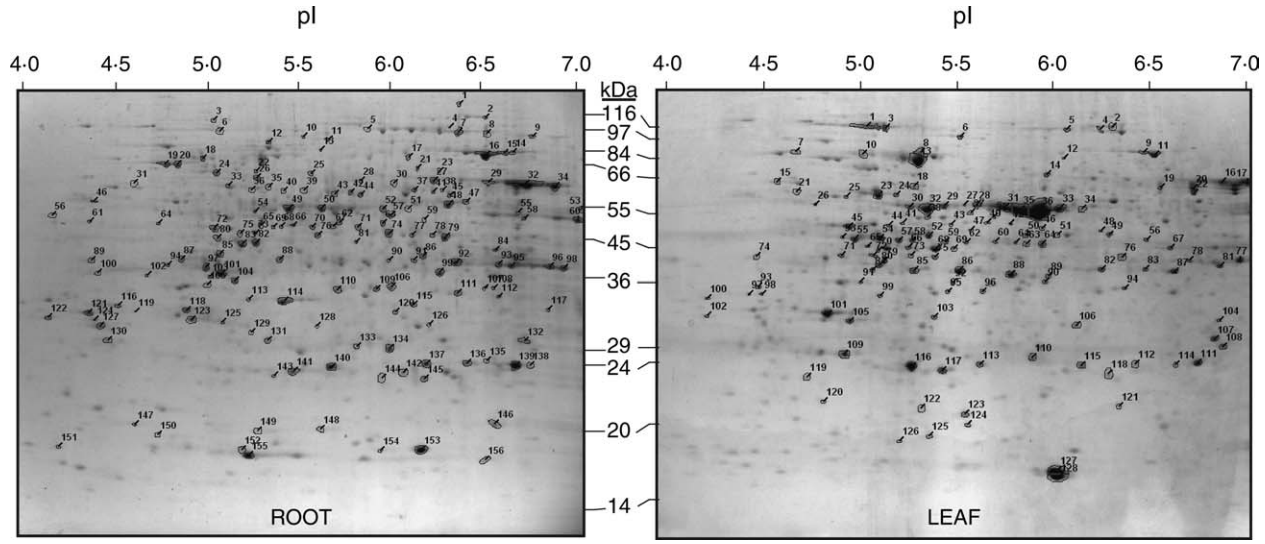

Fig. 1. Two-dimensional gel electrophoretic separation of *Arabidopsis thaliana* developing root and leaf proteins. Total isolated protein (1 mg per gel) was focused on pH 4–7 immobilized pH gradient strips followed by 11–17% linear gradient acrylamide sodium dodecyl sulfate–polyacrylamide gel electrophoresis. Proteins were stained with colloidal Coomassie brilliant blue and gels were imaged by scanning densitometry. The spot boundaries and numbers for every protein analyzed herein are shown.

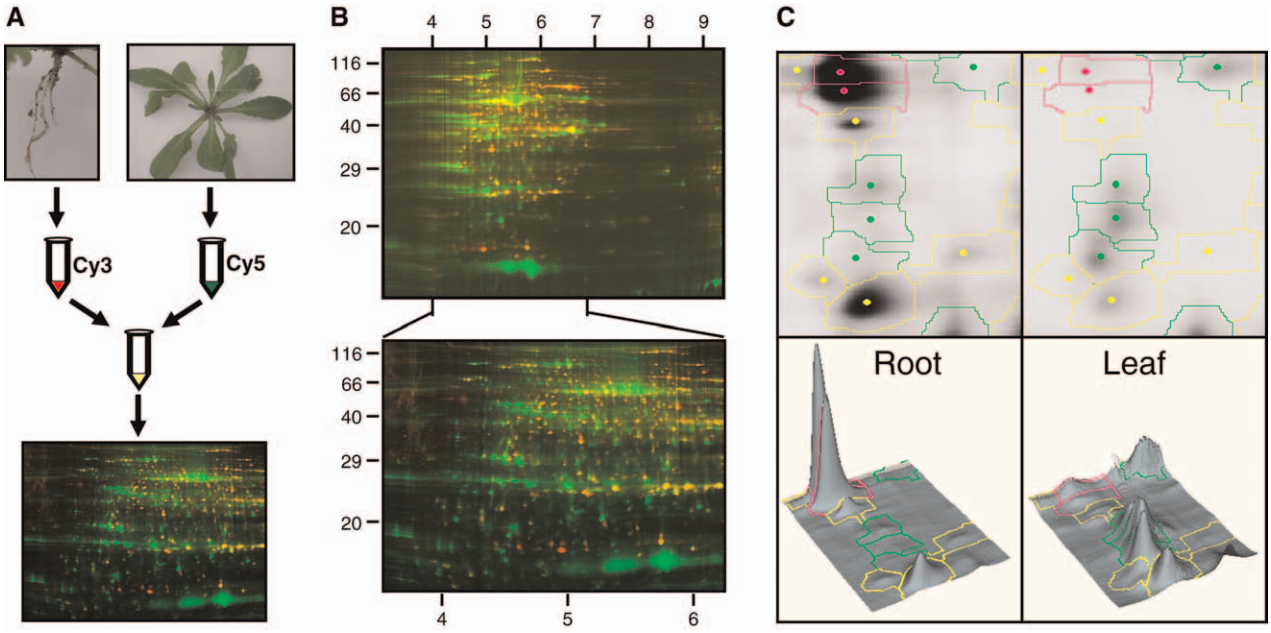

Fig. 2. Difference gel electrophoretic (DIGE) analysis of *Arabidopsis thaliana* root and leaf proteins. (A) Experimental design for DIGE multiplexing of root and leaf samples. Root and leaf proteins (50 μg each) were labeled with Cy3 (red) and Cy5 (green) dyes, respectively. (B) Multiplexed root and leaf samples resolved by two-dimensional (2-D) electrophoresis with pH 3–10 (upper panel) and 4–7 (lower panel) immobilized pH gradient strips. Note that the bulk of root and leaf proteins migrate in the 4–7 pH range. Molecular weight and pI values are shown. (C) Quantification of proteins expressed in roots vs leaves using DeCyder software. Images (16-bit TIFF, grayscale) of separated Cy3 and Cy5 channels were imported into the Difference In-gel Analysis (DIA) component of the DeCyder software suite. A portion of the DIGE gel following DIA analysis is shown along with the corresponding area in three dimensions below. Top panel, gray-scale images of cyanine dye–labeled root and leaf protein samples resolved by pH 4–7 2-D electrophoresis. Relative protein abundance is indicated by colored spot boundaries. Proteins more abundant in roots are bounded by red, more in leaves are bounded by green and equally abundant proteins are bounded by yellow. Lower panels, three-dimensional view of local spot patterns in top panels, offset by approximately 30° for presentation. The three-dimensional views are useful for manual inspection of spot boundaries.

leaf samples over the pH range 3–10 revealed that most proteins had pI values between 4 and 7, and would be optimally resolved with a medium-range IPG strip of pH 4–7 (Fig. 2B, lower panel). A similar observation was made with CBB-stained gels of proteins from roots or leaves (data not shown), therefore all quantitative comparisons were performed using pH 4–7 gels.

Greater proteome coverage was achieved using DIGE

The average number of spot pairs detected from replicate pH 4–7 DIGE gels was 1126, more than twice as many spots as were observed with CBB-stained gels. Quantitative analysis of cyanine dye–labeled protein spots revealed a dynamic range over 200-fold from 2-D gels of leaf proteins, a much broader range than that observed for CBB-stained gels. The greater dynamic range of protein expression observed with CyDye labeling is likely a closer reflection of steady-state protein expression than that observed with CBB staining, because of the limited dynamic range of the latter (Berggren et al. 2000). Duplicate DIGE gels were run with proteins extracted from separate samples (biological replicates). These duplicate gels were analyzed using DeCyder image analysis software (GE Healthcare/Amersham Biosciences), designed specifically for use with DIGE gels. The software uses 16-bit grayscale images for analysis, though spots can be assigned false colors to match those seen in the overlaid gel images. Proteins more abundant in roots are shown in red, those more abundant in leaves are shown in green and those present at similar levels in both samples are shown in yellow (Fig. 2B). Spot boundaries and artifacts were manually evaluated using the three-dimensional field view of the software (Fig. 2C).

The average total number of spots detected on the duplicate DIGE gels varied only slightly and the percentage of changes between root and leaf samples was reproducible as indicated by the low standard deviation values (Table 1). The overall protein abundance differences between roots and leaves are unambiguous, and quantitative analysis of protein levels indicates that 653 spot pairs, representing almost 58% of the total detectable spots, were at least 1.5-fold differentially expressed. Unexpectedly, 188 spot pairs (17% total spots) were at least five-fold different in relative abundance (Table 1).

Table 1. Relative expression of protein spots from coresolved root and leaf samples using Difference Gel Electrophoresis. Root and leaf samples (50 μg each) were labeled with Cy3 or Cy5 dyes, respectively, pooled and resolved by 2-D electrophoresis (pH 4–7 immobilized pH gradient strip), and imaged using a dual photomultiplier laser scanner, which captures a true 16-bit (65 536 gray shades) image. Detection and quantification of spots from biological duplicate gels were performed using DeCyder software (GE Healthcare/Amersham Biosciences). An average of 1126 matched spot pairs was detected. For relative quantification of each spot pair, background fluorescence was subtracted and spot volumes were normalized from each individual image and expressed as a ratio. Fold changes in expression were calculated and tallied; a fold decrease in expression indicates higher expression in roots, whereas a fold increase indicates higher expression in leaves. The percentage of total spots and standard deviations for each class are shown.

Expression difference	Decreased (higher in roots)	Similar	Increased (higher in leaves)
	Number of spots (% of total standard deviation)		
>1.5-fold	200 (17 ± 1)	473 (42 ± 0)	453 (40 ± 1)
>2.0-fold	96 (9 ± 0)	673 (60 ± 1)	357 (32 ± 1)
>3.0-fold	37 (3 ± 1)	833 (74 ± 2)	256 (23 ± 2)
>4.0-fold	18 (2 ± 0)	897 (80 ± 1)	211 (19 ± 1)
>5.0-fold	9 (1 ± 0)	938 (83 ± 2)	179 (16 ± 2)

PMF analysis identified 156 and 128 protein spots from roots and leaves, respectively

The availability of an annotated genome for *A. thaliana* facilitates the use of PMF for protein identification. As a contemporary protein identification approach, PMF is rapid, inexpensive and easily automated (Mooney et al. 2004). To maximize the number of assigned proteins, spots were excised from preparative, CBB-stained gels. The most abundant protein spots (288) were excised from each of the root and leaf CBB-stained gels (576 total spots) for PMF analysis. A total of 156 (54%) proteins spots from roots and 128 (44%) protein spots from leaves were identified using this approach (Supplementary table). In general, the unidentified protein spots were unassigned either because the samples yielded low-quality mass spectra (i.e. few peptide ions or high noise) or did not meet our stringent criteria for protein assignment.

Rigorous acceptance criteria were applied to PMF analyses to minimize false-positive assignments. Minimum threshold values were empirically determined, based upon analysis of standards, for the criteria: mass spectrum quality, minimum number of peptides to match, peptide mass tolerance, MOWSE score and protein coverage. Finally, the sequence-deduced mass of each protein ''hit'' was compared with the relative mass from 2-D gel electrophoresis. In general, theoretical and experimental masses were within a 25% difference, whereas pI value error was frequently outside this range and therefore not considered as a reliable or diagnostic parameter for assessing PMF match quality.

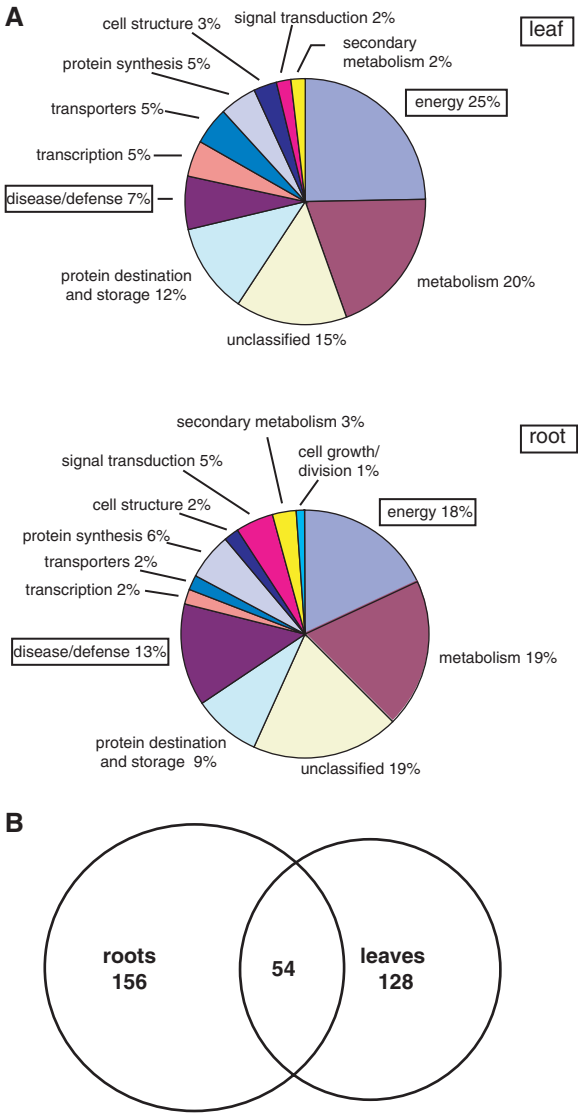

Fig. 3. Classification and overlap of protein assignments from root and leaf samples. (A) Each protein assignment from roots and leaves was classified according to a 15-class nomenclature scheme previously described for plants (Bevan et al. 1998). (B) Venn diagram overlay of protein assignments from roots and leaves. From 156 protein assignments from root samples and 128 from leaves, 54 proteins total had similar function. Area of circles is proportional to the number of protein assignments.

Functional classification of each protein assignment according to the gene nomenclature adopted by Bevan et al. (1998) revealed fundamental differences between root and leaf proteomes (Fig. 3A). For example, disease and defense-related proteins represented 13% of total proteins in roots, whereas in leaves this class was only 7%. Proteins involved in energy production were the most prevalent class in leaves (25%), whereas they represent 18% of total proteins in roots.

Proteins observed in both roots and leaves

Comparison of proteins identified from roots and leaves revealed only 54 spots in common (Fig. 3B), 24 of which correspond to non-redundant protein assignments. The low percentage of common proteins found in both roots and leaves is in agreement with the marked differences between the 2-D gel spot maps and

Table 2. Relative expression of specific protein spot groups identified in both roots and leaves. Proteins identified by peptide mass fingerprinting from Coomassie brilliant blue (CBB)–stained two-dimensional (2-D) gels of both roots and leaves were quantified using Phoretix (Coomassie-stained gels) or DeCyder (cyanine dye) 2-D analysis software. Gene expression, based upon microarray analyses (Stanford Microarray Database, genome-www5.Stanford.edu), are also listed for each assignment. Microarray values are the average of all redundant elements on the slide. Protein spot volumes and transcript abundance are expressed as paired ratios (normalized volume or intensity) of leaves to roots. Protein spots (from CBB-stained gels) that were not unequivocally matched to gels of cyanine dye–labeled samples are noted as unmatched (–).

	Expression ratio (leaf/root)		
Protein function	Coomassie blue	DIGE	Microarray
Root enriched			
Monodehydroascorbate reductase	0.10	–	0.89
S-adenosylmethionine synthase	0.10	0.41	0.62
Fructose-bisphosphate aldolase	0.20	0.25	8.47
6-Phosphogluconate DH	0.28	–	0.46
Gly-rich RNA-binding protein 8	0.30	0.25	0.49
Glutathione *S*-transferase	0.35	0.70	1.38
Annexin	0.37	0.30	1.08
Actin 8	0.42	–	0.42
Myrosinase-binding protein	0.43	–	0.42
Homocysteine *S*-methyltransferase	0.54	0.32	0.69
Similar in roots and leaves			
β-Glucosidase	0.29	1.36	1.89
Unnamed protein product	0.30	1.31	NA[a]
Malate dehydrogenase, cytosolic	0.68	0.75	0.83
Glutathione (GSH)-dependent dehydroascorbate reductase	1.09	0.37	2.06
Glyceraldehyde-3-P dehydrogenase (DH), cytosolic	1.14	0.58	0.90
endoplastic reticulum (ER)-luminal–binding protein	1.39	0.94	0.89
Leaf enriched			
Mitochondrial F1 adenosine 5′-triphosphate (ATP)-synthase β-SU	2.13	6.60	0.97
Clp protease ATP-binding subunit (SU)	4.00	2.51	1.91
Glutamine synthetase	4.35	17.20	0.46
Actin 2/7	4.55	9.27	1.01
RuBisCO large subunit (LSU)	22.50	43.40	14.60[b]

[a]Not present in microarray data.
[b]Small subunit of ribulose-1,5-bisphosphate carboxylase oxygenase (RuBisCO).

the specialized function of these organs. Many of the proteins in common are involved in primary metabolic pathways or cell structure (Table 2). Spot volume calculations indicated that enzymes involved in one-carbon metabolism, *S*-adenosylmethionine synthase and homocysteine *S*-methyltransferase, were more abundant in roots vs leaves. Detoxification-related proteins monodehydroascorbate reductase and glutathione *S*-transferase were also root-enriched, as well as annexin and glycine-rich RNA-binding proteins. In leaves, RuBisCO large subunit, glutamine synthetase and actin 2/7 were prominent, particularly in comparison with roots.

The most abundant protein spot groups, based upon cumulative spot volume, identified from roots and leaves are listed in Table 3. In roots and leaves, these proteins comprised 45 and 63%, respectively, of CBB-staining intensity. Most of these protein species were present in multiple spots differing only by their pI values, suggesting multiple gene products or posttranslational modifications. In the case of RuBisCO large subunit, the high number of spots is partly because of the ''unfocused'' appearance of this prominent protein species (Fig. 1). Roots and leaves had six common predominant proteins, glutathione *S*-transferase, homocysteine *S*-methyltransferase, fructose-bisphosphate aldolase, glyceraldehyde 3-phosphate dehydrogenase, and ATP synthase α- and β-subunits, indicating that these activities are truly constitutively expressed.

Table 3. Catalog of the most abundant proteins expressed in developing *Arabidopsis thaliana* roots and leaves. Abundance of each protein spot in Fig. 1 was quantified from 16-bit TIFF image files using Phoretix two-dimensional Advanced analysis software. Spot volumes were expressed as a percentage of the total volume of all detectable spots and redundant protein assignments were summed for relative volume. Spot numbers, protein assignment and relative volumes are shown for the most abundant protein classes in both roots and leaves.

Spot number	Protein identity	Relative volume
Roots		
30, 32, 34	β-glucosidase	7.7
2, 7, 14, 15, 16	Homocysteine *S*-methyltransferase	7.5
136, 137, 139	Glutathione *S*-transferase, putative	5.9
153, 155	Putative major latex protein	5.6
110, 114, 115	Putative lectin	4.0
63, 80, 140	Monodehydroascorbate reductase-like protein	3.1
49	Mitochondrial F1 ATP-synthase β-SU	2.0
133, 134	L-Ascorbate peroxidase, cytosolic (APX1)	2.0
89, 91, 92	Fructose-bisphosphate aldolase-like protein	2.0
69, 71, 73, 76	*S*-adenosylmethionine synthase	1.7
141	GSH-dependent dehydroascorbate reductase 1	1.8
93, 95, 96, 98	Glyceraldehyde-3-phosphate DH, cytosolic	0.9
45, 48	Mitochondrial F1 ATP-synthase α-SU	0.7
	Total	44.9
Leaves		
14, 28, 31, 32, 34–37, 40	Ribulosebisphosphate carboxylase, LSU	32.8
127, 128	Ribulose bisphosphate carboxylase, SSU	8.0
112–115, 118	Glutathione *S*-transferase	3.0
27, 29, 30, 33	Mitochondrial F1 ATP-synthase β-SU	3.0
85, 86	Fructose-bisphosphate aldolase	3.0
1, 3	Lipoxygenase AtLOX2	2.6
109	Chlorophyll *a*/*b*–binding protein	2.3
23, 24	Mitochondrial F1 ATP-synthase "α-SU	2.1
116	23 kDa polypeptide of oxygen-evolving complex	2.0
64, 77, 78	Glyceraldehyde 3-phosphate dehydrogenase	1.5
8, 10	Homocysteine *S*-methyltransferase	1.4
9, 16, 19, 20, 22	Thioglucosidase	1.0
	Total	62.7

Discussion

It is important to consider that the results from all proteomic analyses are the sum of their parts. For the studies described herein, we have chosen to use a traditional method of protein separation, 2-D electrophoresis, in conjunction with a newer and very sensitive quantitative method of protein spot detection/analysis, DIGE. We recognize that all electrophoresis-based methods tend to underrepresent integral membrane proteins, as well as those that are very large or small, or have extreme isoelectric points. An older method for protein isolation has been used (Hurkman and Tanaka 1986), but it remains widely used and contemporary modifications have not yielded significant improvements (e.g. Natarajan et al. 2005). The use of PMF for identification of protein spots is not ideal, and depends upon a fortuitous distribution of trypsin sites, and the ability to obtain clear ions allowing identification. These various drawbacks notwithstanding, the experimental strategy used herein has yielded a robust and reproducible data set suitable for use in a global, systems biology context (Bevan and Walsh 2005, Glinski and Weckwerth 2006).

Previous proteome investigations of plants have been aimed at cataloging proteins from isolated organelle

fractions including nuclei (Bae et al. 2003), mitochondria (Kruft et al. 2001, Hochholdinger et al. 2004, Millar et al. 2001), chloroplasts (Kleffmann et al. 2004), vacuoles (Carter et al. 2004) and the endoplasmic reticulum (Maltman et al. 2002). Proteomic analysis of chloroplast subfractions has also been successful in defining low-complexity samples including total thylakoids (Friso et al. 2004, Peltier et al. 2000) and thylakoid luminal proteins (Schubert et al. 2002), envelope membranes (Ferro et al. 2002, 2003, Froehlich et al. 2003) and recently a Triton-insoluble chloroplast fraction enriched in protein–protein and protein–nucleic acid complexes (Phinney and Thelen 2005). Relatively fewer plant proteome investigations have been undertaken for quantitative analyses, particularly at the whole organ level (Giavalisco et al. 2005, Koller et al. 2002, Komatsu and Tanaka 2004). Roots and leaves are fundamentally different organs. A better understanding of the major protein composition of these organs will aid our understanding of this specialization, especially in terms of physiological variation (i.e. Renaut et al. 2006). Furthermore, we propose the potential utility of using precise quantitative comparisons to predict differences in intermediary metabolism.

In previous investigations of *M. truncatula* (Watson et al. 2003) and maize (Porubleva et al. 2001), identified proteins were separated into functional categories based upon various classification schemes. Although some of the protein categories differ slightly among the previous papers and those described herein, similar trends are apparent. Energy plus metabolism-related proteins combined comprise 58, 30, and 45% of identified proteins in *M. truncatula*, *Z. mays*, and *A. thaliana* leaves, respectively. A clear trend of higher energy-related protein abundance is also consistent between *M. truncatula* and *A. thaliana*. Maize leaves contain a much higher percentage of proteins annotated as unknown or hypothetical functions (59%) compared with *M. truncatula* (3%) or *A. thaliana* (15%). This might be partly because of evolutionary divergence, or perhaps simply inadequate sequence annotation. Our rate of identification of proteins as unknown or hypothetical is slightly less than the approximately 20% typically reported from studies of *A. thaliana* (Bae et al. 2003, Heazlewood et al. 2004, Giavalisco et al. 2005), possibly because we analyzed only leaves and roots from specific developmental stages. Disease and defense-related proteins were also higher in frequency and relative abundance in *A. thaliana* roots compared with *A. thaliana* leaves. Increased levels of disease and defense proteins in roots vs leaves were also observed in *M. truncatula*, and this is consistent with the barrier function roots serve against soil-borne pathogens (Walker et al. 2003).

Using DIGE simplifies spot matching between protein samples

One of the most difficult challenges in proteomics investigations is quantitative analysis of protein expression. The time-honored approach of 2-D electrophoresis, despite recent improvements, is still fraught with problems in reproducibility and dynamic range of protein detection. An improvement to this technique allows resolution of up to three different protein samples in a single gel by prelabeling with charge-matched, primary amine-reactive cyanine dyes (Alban et al. 2003, Renaut et al. 2006, Rose et al. 2004). Spot matching of diverse protein samples (roots and leaves) proved technically difficult using conventional 2-D gel approaches and application of the DIGE approach greatly simplifies both this and the quantitative analysis (Peck 2005). Like silver-stain protein detection, the CyDyes can be used to detect picogram levels of proteins (Chevalier et al. 2004, Gade et al. 2003). To obtain a higher frequency of protein identification, however, it was necessary to utilize preparative 2-D gels containing 1 mg of protein for spot-excision and subsequent PMF (Fig. 1). The small amounts of protein (50 μg total) analyzed using the DIGE approach, although superior for protein spot resolution, precluded reliable identification by PMF, which requires more material on the MALDI target to obtain high-quality spectra. Ten picomoles of a 50 kDa protein equals 0.5 μg (or 1% of a protein analyzed by DIGE); however, recovery from the gel following trypsin digestion and further processing, especially concentration using a vacuum centrifugal evaporator, is typically approximately 50% (Speicher et al. 2000) making the actual requirement closer to 1 μg. For this reason, CBB-stained gels were used for PMF analyses.

Comparison of CBB and cyanine dyes–stained 2-D gels revealed differences in absolute protein abundance, possibly because of the selective reactivity of N-hydroxysuccinimide-activated cyanine dyes. Coomassie G-250 reportedly binds to basic amino acids including Arg, Tyr, Lys and His (De Moreno et al. 1986), whereas NHS-activated cyanine dyes react exclusively with Lys residues. In addition to absolute expression differences, comparison of root and leaf protein abundance ratios obtained from CBB vs cyanine dye labeling indicated differences in relative abundance calculations between the two detection methods (Table 2). The most contrasting differences were observed with *S*-adenosylmethionine synthase, β-glucosidase and glutamine synthetase. The largest differences between

these two detection methods were observed with proteins that are highly enriched in either roots or leaves. This is in agreement with the previously reported limits in dynamic range for CBB staining (Berggren et al. 2000, Chevalier et al. 2004). Despite some restrictions, DIGE represents a significant improvement over previous protein detection and 2-D electrophoretic-based approaches (Alban et al. 2003, Gade et al. 2003, Kolkman et al. 2005, Rose et al. 2004).

Comparison of transcript vs protein expression in *A. thaliana* roots and leaves

Although there appears to be a good correlation between transcript and protein abundance in *Escherichia coli* (Corbin et al. 2003), global comparisons of yeast, mammalian cells or the archaeon *Methanococcus maripaludis* yielded correlations coefficients of 0.36, 0.48 and 0.24, respectively (Anderson and Seilhamer 1997, Gygi et al. 1999, Xia et al. 2006). A relatively low correlation has also been reported for *A. thaliana* chloroplasts (Baginsky et al. 2005) and pollen (Holmes-Davis et al. 2005, Noir et al. 2005), suggesting a widespread lack of correlation between transcript and protein abundance. The lack of correlation encompasses many factors, including rates of protein and mRNA synthesis, alternative splicing, stability, post-translational modifications and turnover. Nevertheless, oligonucleotide and cDNA microarrays are frequently used for comprehensive profiling of whole organs. Data from cDNA microarray analyses comparing developing roots and leaves of *A. thaliana* were retrieved from the Stanford Microarray Database (http://genome-www5.stanford.edu) for comparison with protein expression data presented herein.

Approximately one-third of the transcript expression data were within 26% variation of the protein expression data (Table 2). The enzymes that displayed the largest discrepancy between transcript and protein abundance were monodehydroascorbate reductase, fructose bisphosphate aldolase, actin, *S*-adenosylmethionine synthase and glutamine synthetase. The overall correlation coefficient for our comparison of CBB-quantified protein data and microarray transcript data was 0.65, whereas the correlation between DIGE and microarray analyses was 0.55. Although these values are slightly better than correlation coefficients previously reported from studies of yeast and mammalian cells, they still indicate significant differences in the results obtained using the two different methods. This finding emphasizes the importance of quantitative proteomics as an integral component of any large-scale systems biology investigations (Glinski and Weckwerth 2006).

A quantitative proteomics-based model of root and leaf metabolism indicates a relatively increased capacity for mitochondrial metabolism in roots

The most abundant class of proteins identified in this root and leaf proteome study of *A. thaliana* are those involved in primary metabolism. This was not unexpected, considering the results from recent proteomic analyses of plant organs (Holmes-Davis et al. 2005, Koller et al. 2002, Liska et al. 2004, Schiltz et al. 2004). However, in contrast to these other reports, the model that we have constructed is based upon the quantitative differences in protein levels in the two organs. Using the data obtained for each CBB-stained spot in Fig. 1, along with the protein identification data (Supplementary table), it was possible to construct a model of the metabolic pathways that predominate root and leaf function (Fig. 4). Based upon these analyses, it appears that the overall contribution of the Krebs cycle is relatively greater in roots than in leaves. In addition to functioning as a mechanism to produce reductant for oxidative phosphorylation, increased expression of specific Krebs-cycle enzymes in roots is a possible adaptation allowing organic acid–mediated uptake of soil phosphorus (Diatloff et al. 2004, Lopez-Bucio et al. 2000, Watanabe and Osaki 2002). The increased abundance of Krebs-cycle enzymes in roots, compared with leaves, could additionally be an adaptation for non-photosynthetic organs to maximize adenosine 5′-triphosphate (ATP) and nicotinamide adenine dinucleotide (reduced) (NADH) production. Mitochondrial oxidative phosphorylation is particularly important for roots because the energy-expensive process of nitrate reduction plays a fundamental biological role in plant growth and development (reviewed in Neuhaus and Emes 2000).

Leaves of course contain large amounts of RuBisCO large and small subunits, and the accumulation of this Calvin-cycle enzyme in leaves is well known. However, the presence of RuBisCO in roots is surprising, because this is a non-photosynthetic organ. Interestingly, a non–Calvin cycle, CO_2-scavenging role for RuBisCO has been demonstrated for developing *Brassica napus* embryos (Schwender et al. 2004). Perhaps RuBisCO performs a similar function in roots considering the increased expression of decarboxylating enzymes of the Krebs cycle.

Concluding remarks

A common misconception is that proteomics research is limited to cataloging the proteins present in a biological sample. However, more recently quantitative proteomic analyses have been used to probe physiological changes (Glinski and Weckwerth 2006, Renaut et al. 2006).

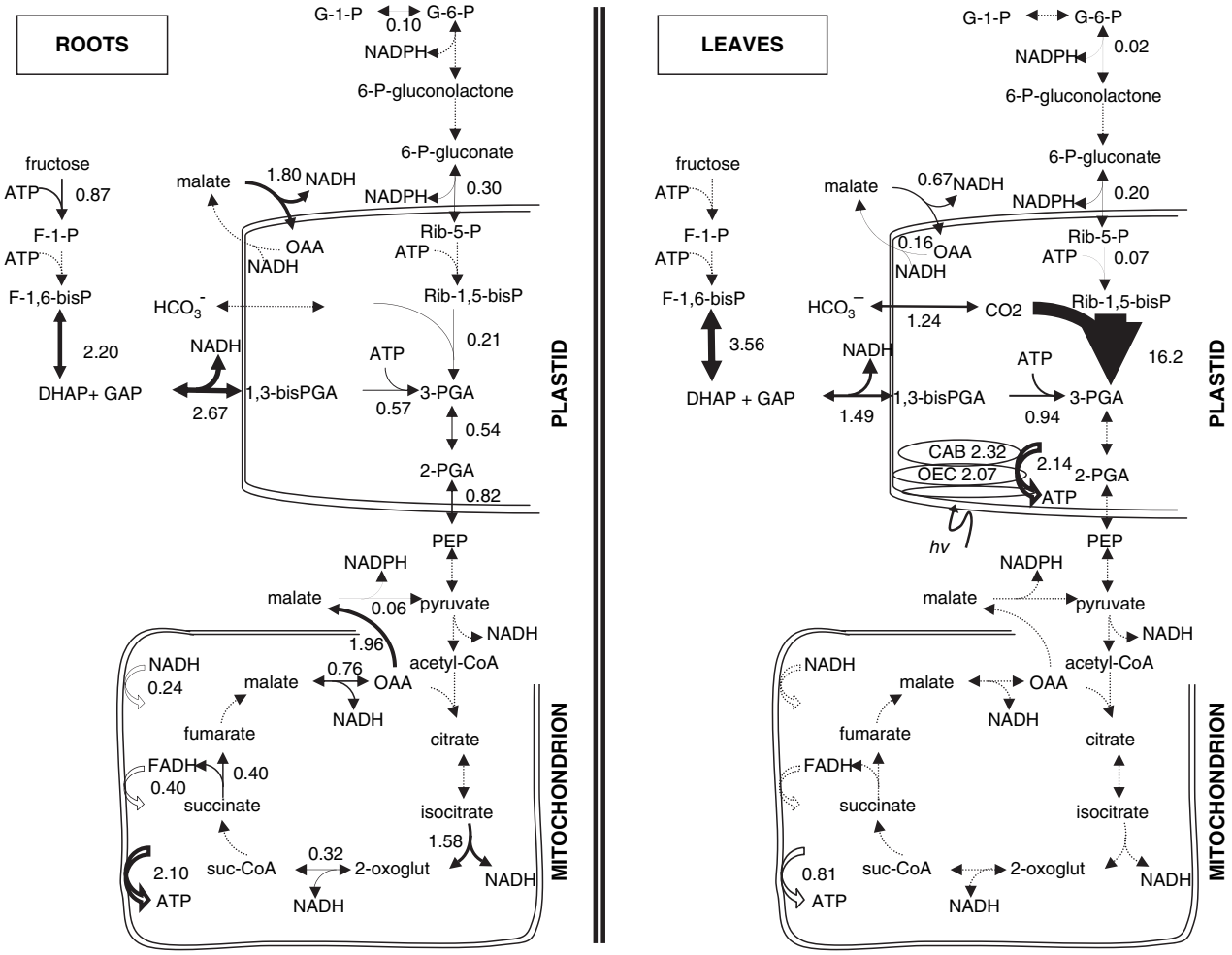

Fig. 4. A model of intermediary metabolism in roots and leaves based upon quantitative protein expression analyses. The arrow thickness and the adjacent numbers for each enzymatic step are proportional to the spot volume from the Coomassie brilliant blue–quantified two-dimensional (2-D) gels. When multiple isoforms for the same protein were detected the values were added. Reactions that were not detected are indicated with dashed lines. Abbreviations: ATP, adenosine triphosphate; CAB, chlorophyll a/b-binding protein; OEC, oxygen evolving complex; NADH, nicotinamide adenine dinucleotide (reduced); NADPH, nicotinamide adenine dinucleotide phosphate (reduced); OAA, oxaloacetic acid; suc-CoA, succinyl-coenzyme A; 2-oxoglut, 2-oxoglutarate; PEP, phosphoenolpyruvate; PGA, phosphoglyceric acid; DHAP, dihydroxyacetone phosphate; F-1-P, fructose-1-phosphate; Rib-5-P, ribulose-5-phosphate.

Herein we propose the use of quantitative proteomic data, obtained from high-resolution 2-D gels, as the basis for metabolic predictions. Such an application should have widespread application. Additional refinement of the high-resolution 2-D proteome maps will facilitate future comparative profiling investigations in areas such as development and stress responses. Furthermore, changes in protein levels caused by a wide range of genetic differences can be rapidly assayed with the benefit of 2-D proteome maps.

We have noted herein the quantitative discrepancy arising from transcript vs protein abundance analyses. Although measurement of transcript abundance provides much useful information (Donson et al. 2002, Peck 2005), we feel that high-resolution proteomic analyses are more appropriate for metabolic predictions, whereas recognizing that results from metabolite profiling (Fiehn and Weckwerth 2003, Kopka et al. 2005) and flux analyses (Fernie et al. 2005) will additionally be necessary before we can approximate the virtual plant.

Supplementary material

The following material is available to download from www.blackwell-synergy.com/doi/abs/10.1111/j.1399-3054.2006.00746.x

Appendix S1. Proteins identified from 2-D gels of *A. thaliana* roots and leaves.

References

Agrawal GK, Yonekura M, Iwahashi Y, Iwahashi H, Rakwal R (2004) System, trends and perspectives of proteomics in dicot plants. Part I: technologies in proteome establishment. J Chromatogr B 815: 109–123

Alban A, David SO, Bjorkesten L, Andersson C, Sloge E, Lewis S, Currie I (2003) A novel experimental design for comparative two-dimensional gel analysis: two-dimensional difference gel electrophoresis incorporating a pooled internal standard. Proteomics 3: 36–44

Anderson L, Seilhamer J (1997) A comparison of selected mRNA and protein abundances in human liver. Electrophoresis 18: 533–537

Arabidopsis Genome Initiative (2000) Analysis of the genome sequence of the flowering plant *Arabidopsis thaliana*. Nature 408: 796–813

Bae MS, Cho EJ, Choi E-Y, Park OK (2003) Analysis of the *Arabidopsis* nuclear proteome and its response to cold stress. Plant J 36: 652–663

Baginsky S, Kleffmann T, von Zychlinski A, Gruissem W (2005) Analysis of shotgun proteomics and RNA profiling data from *Arabidopsis* thaliana chloroplasts. J Proteome Res 4: 637–640

Berggren K, Chernokalskaya E, Steinberg TH, Kemper C, Lopez MF, Diwu Z, Haugland RP, Patton WF (2000) Background-free, high-sensitivity staining of proteins in one- and two-dimensional sodium dodecyl sulfate–polyacrylamide gels using a luminescent ruthenium complex. Electrophoresis 21: 2509–2521

Bevan M, Walsh S (2005) The *Arabidopsis* genome: a foundation for plant research. Genome Res 15: 1632–1642

Bevan M, Bancroft I, Bent E, Love K, Goodman H, Dean C, Bergkamp R, Dirkse et al (1998) Analysis of 1.9 Mb of contiguous sequence from chromosome 4 of *Arabidopsis thaliana*. Nature 391: 485–488

Byrne ME (2005) Networks in leaf development. Curr Opin Plant Biol 8: 59–66

Carter C, Pan S, Zouhar J, Avila EL, Girke T, Raikhel NV (2004) The vegetative vacuole proteome of *Arabidopsis* thaliana reveals predicted and unexpected proteins. Plant Cell 16: 3285–3303

Chevalier F, Rofidal V, Vanova P, Bergoin A, Rossignol M (2004) Proteomic capacity of recent fluorescent dyes for protein staining. Phytochemistry 65: 1499–1506

Corbin RW, Paliy O, Yang F, Shabanowitz J, Platt M, Lyons CE Jr, Root K, McAuliffe J, Jordan MI, Kustu S, Soupene E, Hunt DF (2003) Toward a protein profile of *Escherichia coli*: comparison to its transcription profile. Proc Natl Acad Sci USA 100: 9232–9237

De Moreno MR, Smith JF, Smith RV (1986) Mechanism studies of Coomassie blue and silver staining of proteins. J Pharm Sci 75: 907–911

Diatloff E, Roberts M, Sanders D, Roberts SK (2004) Characterization of anion channels in the plasma membrane of *Arabidopsis* epidermal root cells and the identification of a citrate-permeable channel induced by phosphate starvation. Plant Physiol 136: 4136–4149

Donson J, Fang Y, Espiritu-Santo G, Xing W, Salazar A, Miyamoto S, Armendarez V, Volkmuth W (2002) Comprehensive gene expression analysis by transcript profiling. Plant Mol Biol 48: 75–97

Fernie AR, Geigenberger P, Stitt M (2005) Flux an important, but neglected, component of functional genomics. Curr Opin Plant Biol 8: 174–182

Ferro M, Salvi D, Riviere-Rolland H, Vermat T, Seigneurin-Berny D, Grunwald D, Garin J, Joyard J, Rolland N (2002) Integral membrane proteins of the chloroplast envelope: identification and subcellular localization of new transporters. Proc Natl Acad Sci USA 99: 11487–11492

Ferro M, Salvi D, Brugiere S, Miras S, Kowalski S, Louwagie M, Garin J, Joyard J, Rolland N (2003) Proteomics of the chloroplast envelope membranes from *Arabidopsis thaliana*. Mol Cell Proteomics 2: 325–345

Fiehn O, Weckwerth W (2003) Deciphering metabolic networks. FEBS J 270: 579–588

Friso G, Giacomelli L, Ytterberg AJ, Peltier JB, Rudella A, Sun Q, Wijk KJ (2004) In-depth analysis of the thylakoid membrane proteome of *Arabidopsis thaliana* chloroplasts: new proteins, new functions, and a plastid proteome database. Plant Cell 16: 478–499

Froehlich JE, Wilkerson CG, Ray WK, McAndrew RS, Osteryoung KW, Gage DA, Phinney BS (2003) Proteomic study of the *Arabidopsis thaliana* chloroplastic envelope membrane utilizing alternatives to traditional two-dimensional electrophoresis. J Proteome Res 2: 413–425

Gade D, Thiermann J, Markowsky D, Rabus R (2003) Evaluation of two-dimensional difference gel electrophoresis for protein profiling. J Mol Microbiol Biotechnol 5: 240–251

Giavalisco P, Nordhoff E, Kreitler T, Klöppel K-D, Lehrach H, Klose J, Gobom J (2005) Proteome analysis of *Arabidopsis thaliana* by two-dimensional gel electrophoresis and matrix-assisted laser desorption/ionization-time of flight mass spectrometry. Proteomics 5: 1902–1913

Glinski M, Weckwerth W (2006) The role of mass spectrometry in plant systems biology. Mass Spectrom Rev 25: 173–214

Görg A, Weiss W, Dunn MJ (2004) Current two-dimensional electrophoresis technology for proteomics. Proteomics 4: 3665–3685

Gygi SP, Rochon Y, Franza BR, Aebersold R (1999) Correlation between protein and mRNA abundance in yeast. Mol Cell Biol 19: 1720–1730

Hajduch M, Ganapathy A, Stein JW, Thelen JJ (2005) A systematic proteomic study of seed filling in soybean. Establishment of high-resolution two-dimensional reference maps, expression profiles, and an interactive proteome database. Plant Physiol 137: 1397–1419

Heazlewood JL, Tonti-Filippini JS, Gout AM, Day DA, Whelan J, Millar AH (2004) Experimental analysis of the *Arabidopsis* mitochondrial proteome highlights signaling and regulatory components, provides assessment of targeting prediction programs, and indicates plant-specific mitochondrial proteins. Plant Cell 16: 241–256

Hochholdinger F, Guo L, Schnable PS (2004) Cytoplasmic regulation of the accumulation of nuclear-encoded proteins in the mitochondrial proteome of maize. Plant J 37: 199–208

Holmes-Davis R, Tanaka CK, Vensel WH, Hurkman WJ, McCormick S (2005) Proteome mapping of mature pollen of *Arabidopsis thaliana*. Proteomics Oct 24 [Epub ahead of print]

Hurkman WJ, Tanaka CK (1986) Solubilization of plant membrane proteins for analysis by two-dimensional gel electrophoresis. Plant Physiol 81: 802–806

Kleffmann T, Russenberger D, von Zychlinski A, Christopher W, Sjolander K, Gruissem W, Baginsky S (2004) The *Arabidopsis thaliana* chloroplast proteome reveals pathway abundance and novel protein functions. Curr Biol 14: 354–362

Kochian L (2000) Molecular physiology of mineral nutrient acquisition, transport, and utilization. In: Buchanan BB, Gruissem W, Jones RL (Eds), Biochemistry and Molecular Biology of Plants. American Society for Plant Physiology, Rockville, MD, pp 1204–1249

Kolkman A, Dirksen EH, Slijper M, Heck AJ (2005) Double standards in quantitative proteomics: direct comparative assessment of difference in gel electrophoresis and metabolic stable isotope labeling. Mol Cell Proteomics 4: 255–266

Koller A, Washburn MP, Lange BM, Andon NL, Deciu C, Haynes PA, Hays L, Schieltz D, Ulaszek R, Wei J, Wolters D, Yates JR 3rd (2002) Proteomic survey of metabolic pathways in rice. Proc Natl Acad Sci USA 99: 11969–11974

Komatsu S, Tanaka N (2004) Rice proteome analysis: a step toward functional analysis of the rice genome. Proteomics 4: 938–949

Kopka J, Schauer N, Krueger S, Birkemeyer C, Usadel B, Bergmuller E, Dormann P, Weckwerth W, Gibon Y, Stitt M, Willmitzer L, Fernie AR, Steinhauser D (2005) GMD@CSB.DB: the Golm Metabolome Database. Bioinformatics 21: 1635–1638

Kruft V, Eubel H, Jansch L, Werhahn W, Braun HP (2001) Proteomic approach to identify novel mitochondrial proteins in *Arabidopsis*. Plant Physiol 127: 1694–1710

Liska AJ, Shevchenko A, Pick U, Katz A (2004) Enhanced photosynthesis and redox energy production contribute to salinity tolerance in Dunaliella as revealed by homology-based proteomics. Plant Physiol 136: 2806–2817

Lopez-Bucio J, de La Vega OM, Guevara-Garcia A, Herrera-Estrella L (2000) Enhanced phosphorus uptake in transgenic tobacco plants that overproduce citrate. Nat Biotechnol 18: 450–453

Malkin R, Niyogi K (2000) Photosynthesis. In: Buchanan BB, Gruissem W, Jones RL (Eds), Biochemistry and Molecular Biology of Plants. American Society for Plant Physiology, Rockville, MD, pp 568–628

Maltman DJ, Simon WJ, Wheeler CH, Dunn MJ, Wait R, Slabas AR (2002) Proteomic analysis of the endoplasmic reticulum from developing and germinating seed of castor (*Ricinus communis*). Electrophoresis 23: 626–639

Millar AH, Sweetlove LJ, Giege P, Leaver CJ (2001) Analysis of the *Arabidopsis* mitochondrial proteome. Plant Physiol 127: 1711–1727

Mooney BP, Krishnan HB, Thelen JJ (2004) High-throughput peptide mass fingerprinting of soybean seed protein: automated workflow and utility of UniGene expressed sequence tag databases for protein identification. Phytochemistry 65: 1733–1744

Natarajan S, Xu C, Caperna TJ, Garrett WM (2005) Comparison of protein solubilization methods suitable for proteomic analysis of soybean seed proteins. Anal Biochem 342: 214–220

Neuhaus HE, Emes MJ (2000) Nonphotosynthetic metabolism in plastids. Annu Rev Plant Physiol Plant Mol Biol 51: 111–140

Noir S, Brautigam A, Colby T, Schmidt J, Panstruga R (2005) A reference map of the *Arabidopsis thaliana* mature pollen proteome. Biochem Biophys Res Commun 337: 1257–1266

Pappin DJC, Hojrup P, Bleasby AJ (1993) Rapid identification of proteins by peptide-mass fingerprinting. Curr Biol 3: 327–332

Peck SC (2005) Update on proteomics in *Arabidopsis*. Where do we go from here? Plant Physiol 138: 591–599

Peltier J-B, Friso G, Kalume DE, Roepstorff P, Nilsson F, Adamska I, van Wijk KJ (2000) Proteomics of the chloroplast: systematic identification and targeting analysis of luminal and peripheral thylakoid proteins. Plant Cell 12: 319–341

Phinney BS, Thelen JJ (2005) Proteomic characterization of a Triton-insoluble fraction from chloroplasts defines a novel group of proteins associated with macromolecular structures. J Proteome Res 4: 497–506

Porubleva L, Velden KV, Kothari S, Oliver DJ, Chitnis PR (2001) The proteome of maize leaves: use of gene sequences and expressed sequence tag data for identification of proteins with peptide mass fingerprints. Electrophoresis 22: 1724–1738

Renaut J, Hausman J-F & Wisniewski ME (2006) Proteomics and low-temperature studies: bridging the gap between gene expression and metabolism. Physiol Plant 126: 97–109

Rose JKC, Bashir S, Giovannoni JJ, Jahn MM, Saravanan RS (2004) Tackling the plant proteome: practical approaches, hurdles and experimental tools. Plant J 39: 715–733

Schiltz S, Gallardo K, Huart M, Negroni L, Sommerer N, Burstin J (2004) Proteome reference maps of vegetative tissues in pea. An investigation of nitrogen mobilization from leaves during seed filling. Plant Physiol 135: 2241–2260

Schubert M, Petersson UA, Haas BJ, Funk C, Schroder WP, Kieselbach T (2002) Proteome map of the chloroplast lumen of *Arabidopsis thaliana*. J Biol Chem 277: 8354–8365

Schwender J, Goffman F, Ohlrogge JB, Shachar-Hill Y (2004) Rubisco without the Calvin cycle improves the carbon efficiency of developing green seeds. Nature 432: 779–782

Somerville C, Koornneef M (2002) A fortunate choice: the history of *Arabidopsis* as a model plant. Nat Rev Genet 3: 883–889

Speicher KD, Kolbas O, Harper S, Speicher DW (2000) Systematic analysis of peptide recoveries from in-gel digestions for protein identifications in proteome studies. J Biomol Tech 11: 74–86

Ueda M, Koshino-Kimura Y, Okada K (2005) Stepwise understanding of root development. Curr Opin Plant Biol 8: 71–76

Walker TS, Bais HP, Grotewold E, Vivanco JM (2003) Root exudation and rhizosphere biology. Plant Physiol 132: 44–51

Watanabe T, Osaki M (2002) Role of organic acids in aluminum accumulation and plant growth in *Melastoma malabathricum*. Tree Physiol 22: 785–792

Watson BS, Asirvatham VS, Wang L, Sumner LW (2003) Mapping the proteome of barrel medic (*Medicago truncatula*). Plant Physiol 131: 1104–1123

Xia Q, Hendrickson EL, Zhang Y, Wang T, Taub F, Moore BC, Porat I, Whitman WB, Hackett M, Leigh JA (2006) Quantitative proteomics of the archaeon *Methanococcus maripaludis* validated by microarray analysis and real time PCR. Mol Cell Proteomics Feb 24 [Epub ahead of print]

Edited by P. Gardeström